Comments on the imaging condition

John C. Bancroft

ABSTRACT

The processing of seismic data often uses an imaging condition where an upward propagating waveform is correlated with a downgoing waveform to estimate reflectivity. The cross correlation includes multiple energy that produces a low frequency noise that contaminates a migrated imaging. This noise can be removed by a low cut filter that is counter to the requirement of low frequencies that are required for full waveform inversion. I demonstrate a simplified process that eliminates the low frequency noise.

INTRODUCTION

The cross-correlation process is demonstrated using a 1D problem with three velocity layers. A wavelet is induced into the model which is then reflected and transmitted at the velocity boundaries with correct amplitudes that are defined by the vertical incident equations. Cross-correlations of the forward modelled data with back propagated data (using migration) display a low frequency noise that is at a constant level between the apparent reflections.

THEORY

Accurate wave propagation is a difficult task due to using finite difference equations to approximate the first and second derivatives of the wave-equation. Small sample intervals in time and space are required to prevent grid distortion and amplitude errors. When the velocities vary, a modified form of the equation is required for accurate propagation across boundaries. The interface must also be continuous to prevent aliasing of the model, but reasonably short enough with spatial frequencies high enough to be greater than those of the incident waves. These properties are discussed in a companion paper "Modelling with finite difference approximations to the wave-equation" included in in this Report.

MODEL

The 1D model contains three areas with different velocities, 1,000, 2,000 and 900 m/s as illustrated in Fig. 1a, and the corresponding reflectivity in (b).

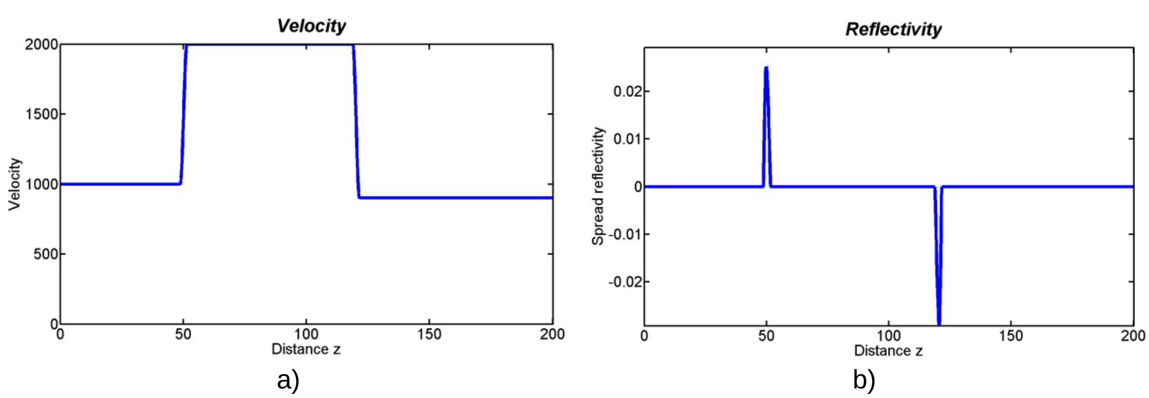

Fig. 1: Part a) shows the velocity model, and b) the reflectivity.

The data are processed with a velocity varying wave-equation, with a three point finite difference approximations to the first and second derivatives. Accurate space and time sampling interval ranged from 0.031 to 2.0 m, and 1 to 0.015625 ms. The width of the transition zone was a raised cosine shape with 21 samples. The surface boundary at z = 0 was totally reflecting and the basement at z_{Max} was totally absorbing.

Forward model

The forward model was created using sample increments of 0.125 m and 0.0625 msec. A three dimensional view of the data is displayed in Figure 2. Note the amplitudes of the incident waves, the reflected waves, and the surface and interbed multiples.

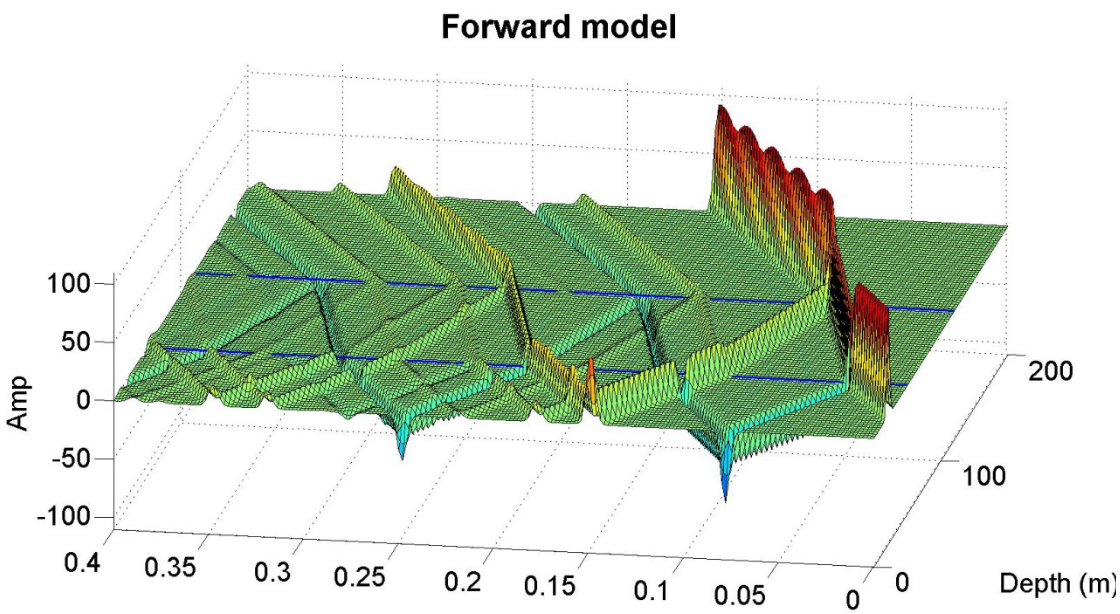

Fig. 2: Three dimensional display of the forward model.

The data in the forward model can be recreated using reverse time or downward continued processes if boundary values were preserved. However, with surface seismic, only data recorded at the surface is available. Recreation of the wavefield using only the surface data follows.

A model of the downward propagating incident wavefield is created by a selective window.

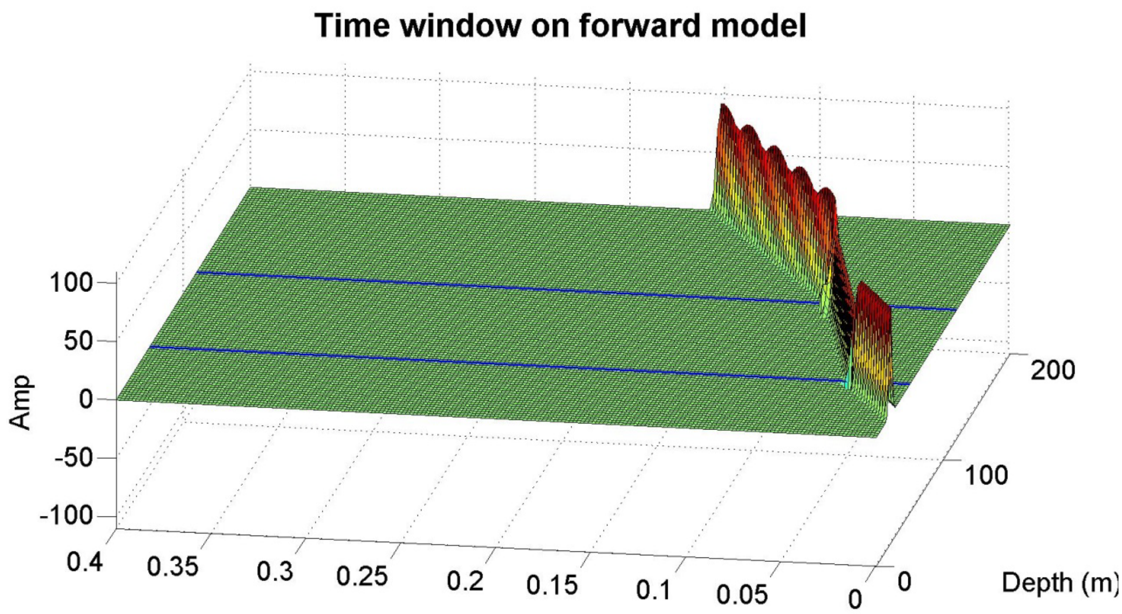

Fig. 3: Window on the forward model.

Recreation of the wavefield using only the surface data

The first example is a recreated wavefield using the reverse time process.

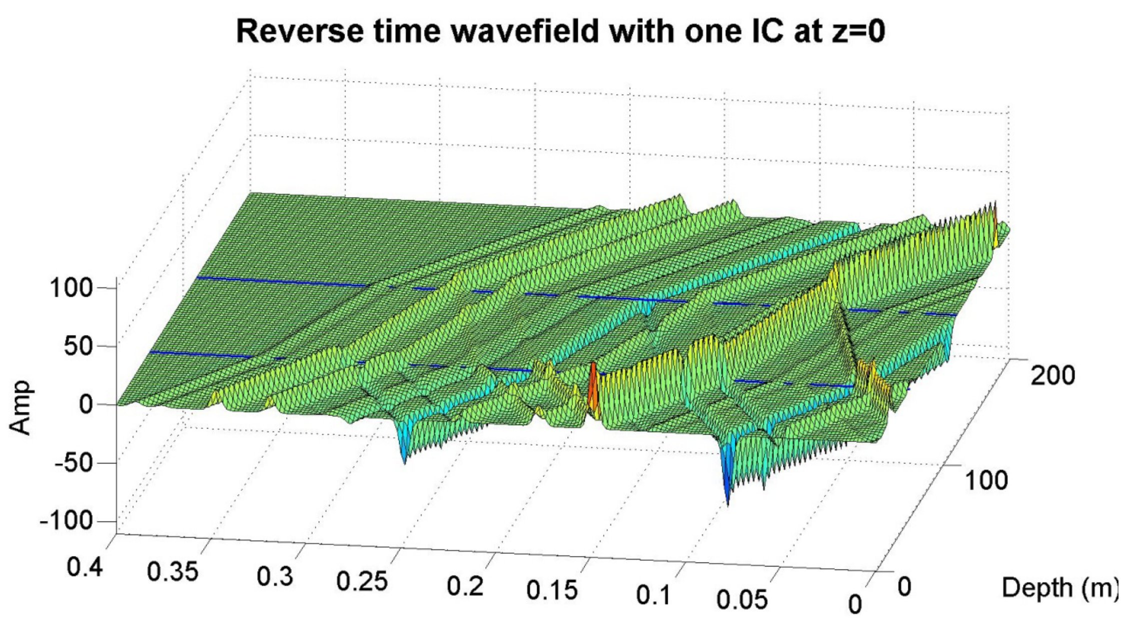

Fig. 4: Recreated wavefield using the reverse time process.

The following figure was created using downward continuation with a finite difference solution to the full wave equation.

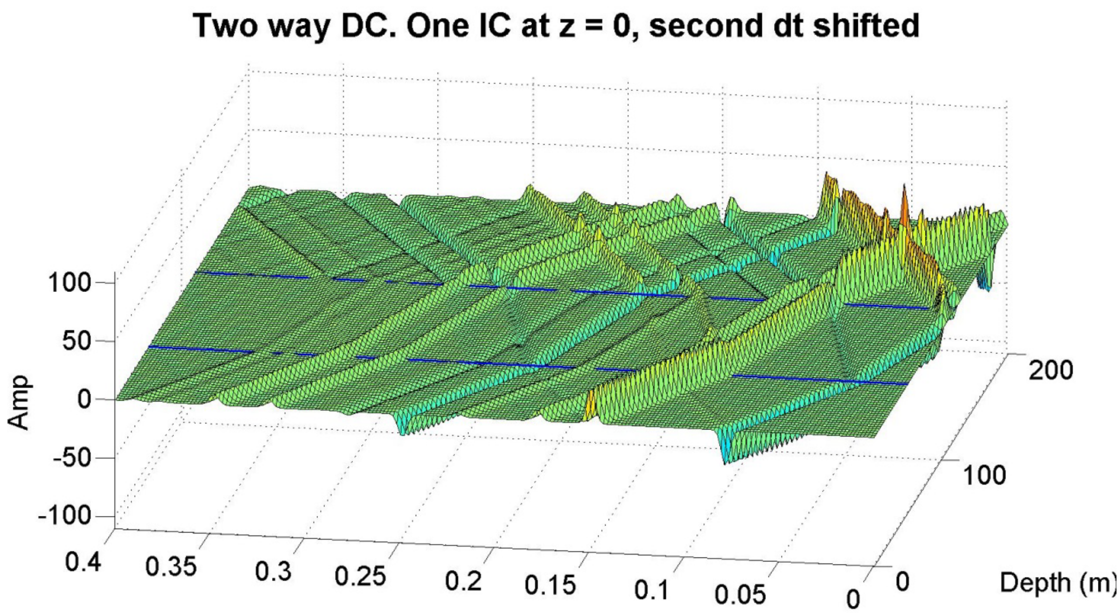

Fig. 5: Wavefield recreated with downward continuation.

The third recreated wavefield was created using downward continuation with the phase shift method.

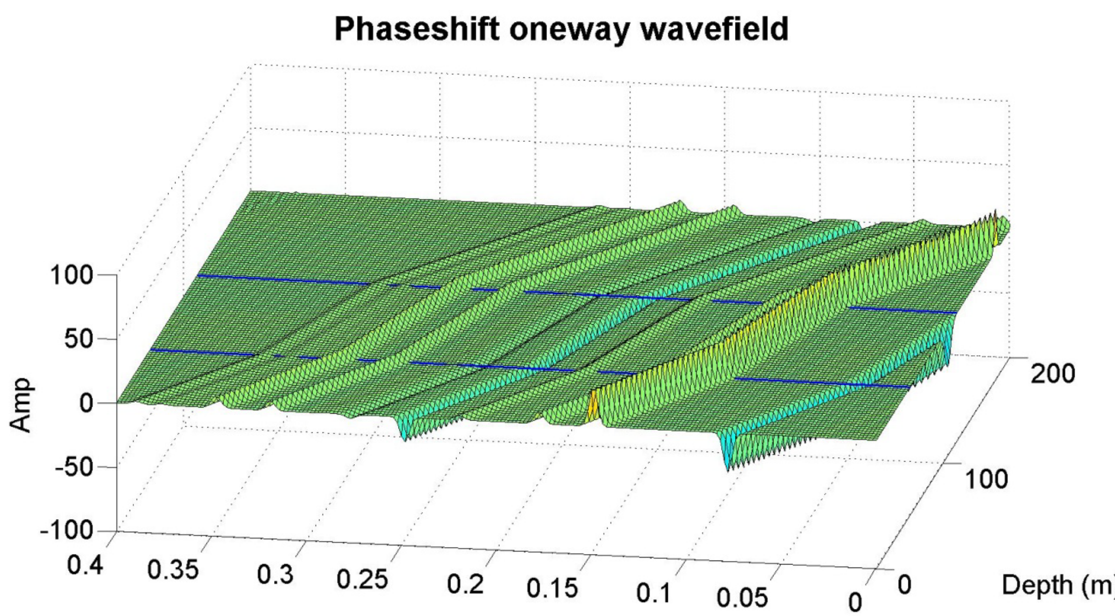

Fig. 6: Recreated wavefield using the downward continuation phase-shift method.

A primary only reconstruction of the wavefield of the phase shift data is shown in Figure 7.

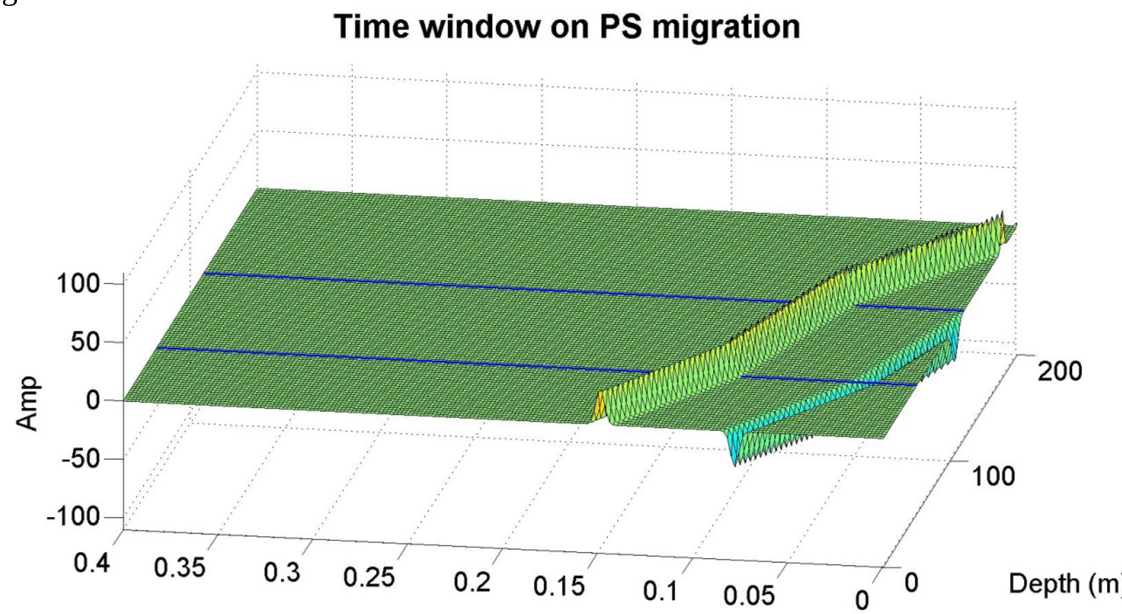

Fig. 7: Only primaries are reconstructed using the phase shift method.

Cross-correlations

The following figures show a number of cross-correlation (CC) using the above data. The first is a CC between the complete forward model (FM) and the complete reverse time using all boundary information. Note the constant levels of amplitudes between the reflection events. This low frequency is removed with low pass filters, contrary to the expectations required for full-waveform-inversion.

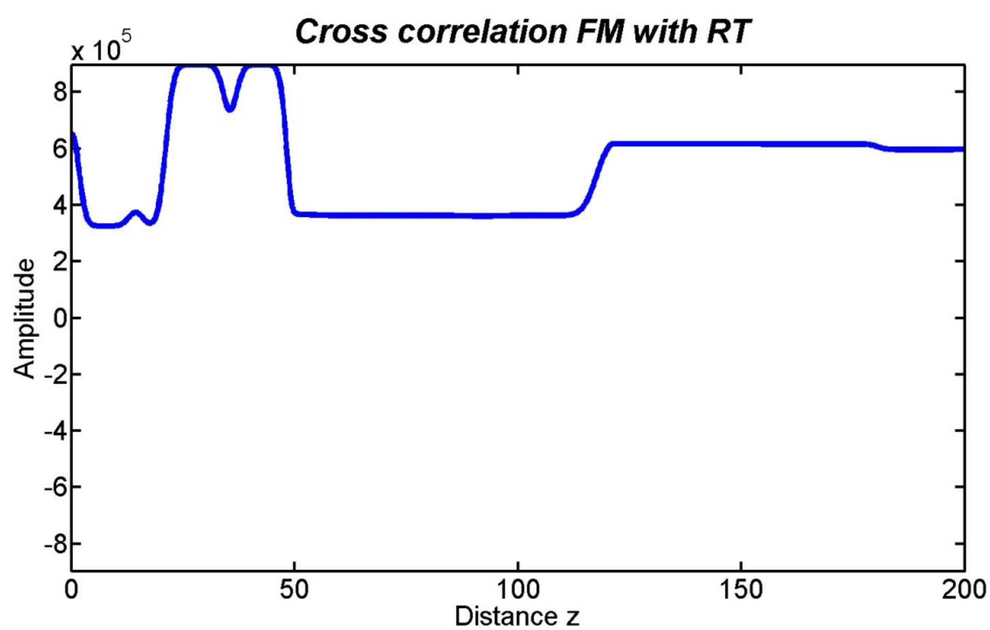

Fig. 8: CC of the full forward model with the full RT using all boundary information.

The next CC shows results when the data used for reconstructing the wavefield uses only the surface seismic for the RT algorithm

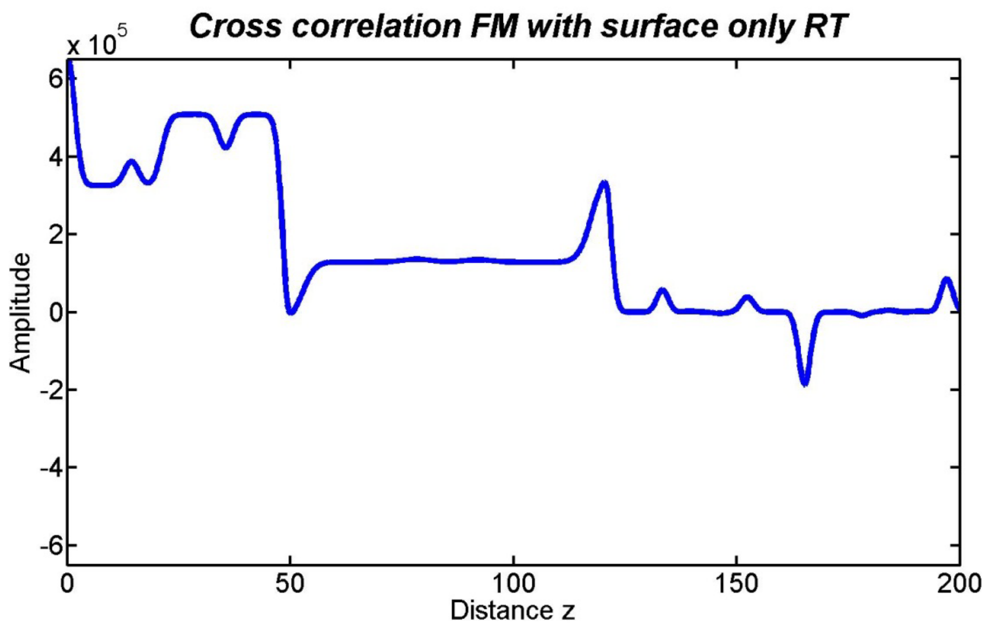

Fig. 9: CC of the forward model with RT using only the surface seismic.

Next is the CC with the phase-shift algorithm

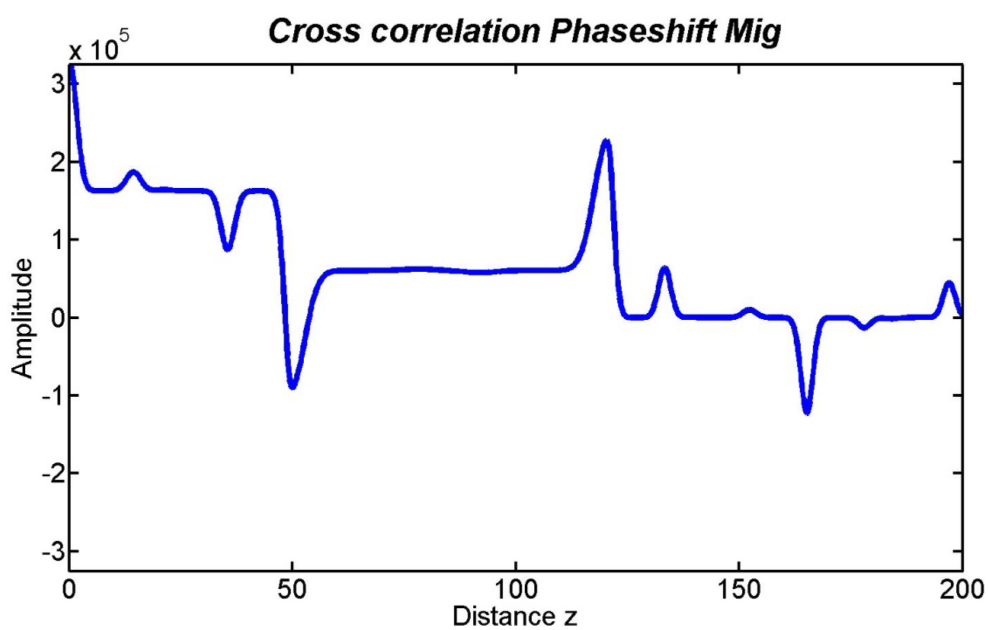

Fig. 10: CC of the FW with the phase-shift algorithm.

The final image uses only the primaries created with the phase-shift method, cross-correlated with a forward model of the down propagating incident wave field.

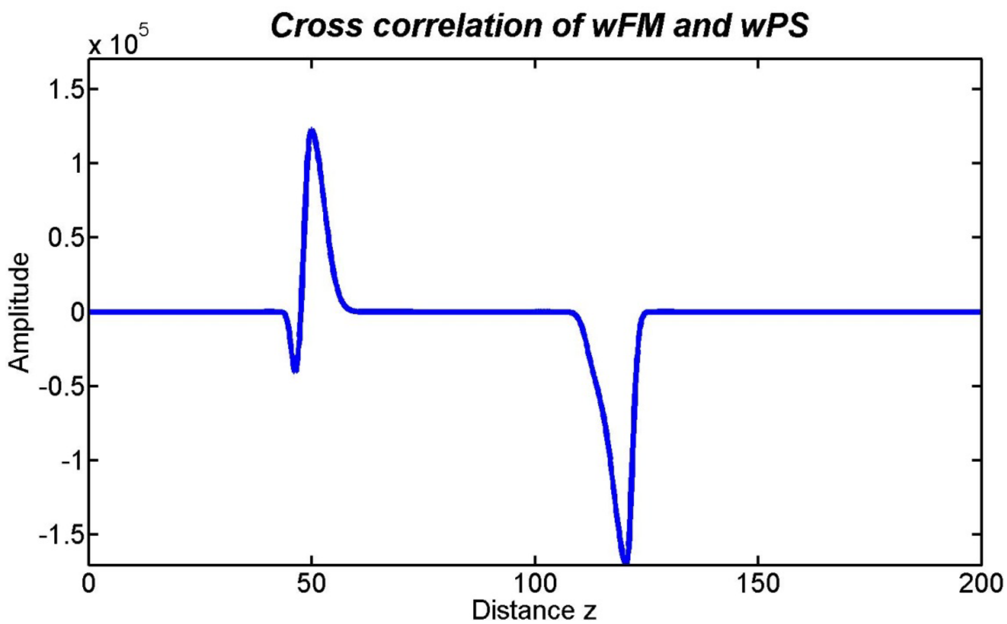

Fig. 11: CC of the windowed forward model with the primary only PS.

COMMENTS AND CONCLUSIONS

Wavefield modelling with one dimension was demonstrated using numerous conditions that replicate the seismic imaging condition. Care must be taken with these examples when extrapolating full dimensional seismic data. However they do indicate that the low frequency noise that plagues the process is a result of the multiple energy. Removal of the multiple energy and using only the downward incident energy produces a reflectivity that matches the true reflectivity.

The wavelet used (Gausian) contained zero frequency energy that allowed the estimated reflectivity to contain zero frequency energy. Typical wavelet with no DC energy will not create an estimated reflectivity with zero frequency. A more realistic example is shown in the appendix, Figure 13.

The examples used a wave-equation that allowed the velocities to vary laterally.

ACKNOWLEDGEMENTS

We thank the sponsors of CREWES for their support. We also gratefully acknowledge support from NSERC (Natural Science and Engineering Research Council of Canada) through the grant CRDPJ 379744-08.

APPENDIX

To illustrate the need for high resolution sample increments, values of 1 m and 0.5 msec were used to create the following image of the wavefield. Compare these result with that of Figure 2 which used sample increments of 0.125 m, and 0.0625 msec. Note the poor amplitudes on the reflection but also the grid dispersion at the greater depths of the downgoing incident wavelet.

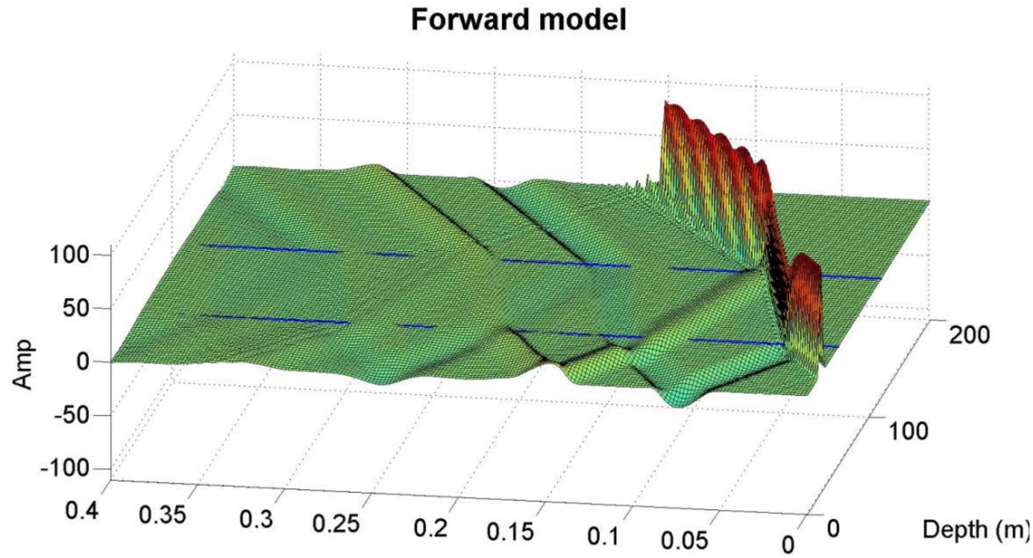

Fig. 12:: Forward model using course sample increments.

The estimated reflectivity using a wavelet with non-zero frequency energy is shown in Figure 13.

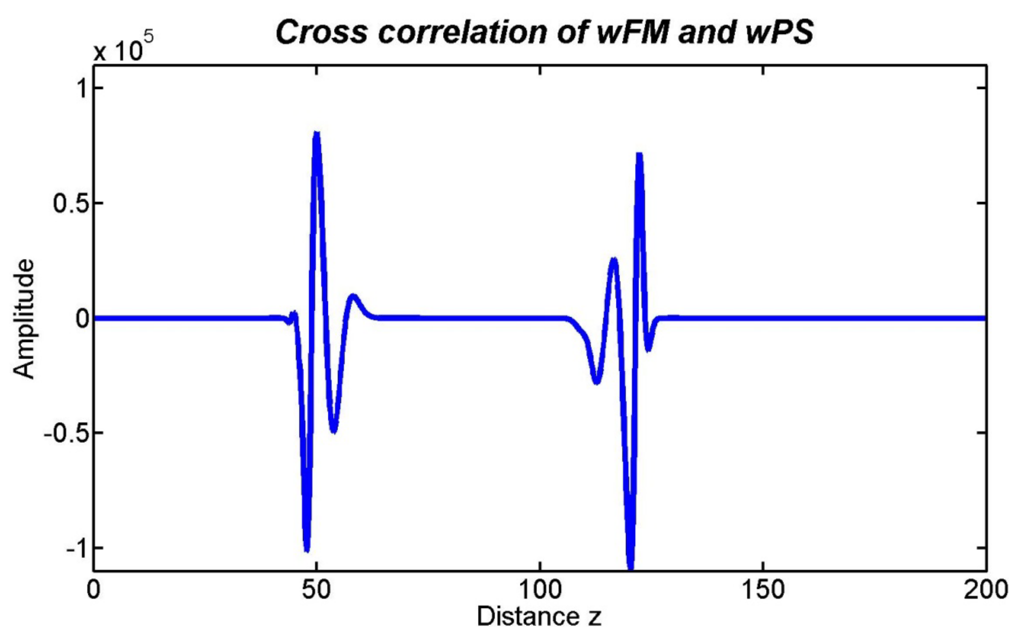

Fig. 13: Reflectivity using a wavelet with no zero frequency energy.